END

FILMED

DTIC

MICROCOPY RESOLUTION TEST CHART
NATIONAL BUREAU OF STANDARDS-1963-A

DNA-TR-81-48

AD A 123560

INSTRUMENTATION AND DATA ACQUISITION FOR SATELLITE TESTING IN NUCLEAR ENVIRONMENTS

Bhagwant Samyal
Walter Naumann
Effects Technology, Incorporated
5383 Hollister Avenue
Santa Barbara, California 93111

30 June 1982

Technical Report

CONTRACT No. DNA 001-81-C-0219

APPROVED FOR PUBLIC RELEASE;
DISTRIBUTION UNLIMITED.

DTIC FILE COPY

Prepared for
    Director
DEFENSE NUCLEAR AGENCY
Washington, DC 20305

DTIC
ELECTE
JAN 20 1983

A

83 01 20 001

UNCLASSIFIED

REPORT DOCUMENTATION PAGE		READ INSTRUCTIONS BEFORE COMPLETING FORM
1. REPORT NUMBER DNA-TR-81-48	2. GOVT ACCESSION NO. AD-A123 560	3. RECIPIENT'S CATALOG NUMBER
4. TITLE (and Subtitle) INSTRUMENTATION AND DATA ACQUISITION FOR SATELLITE TESTING IN NUCLEAR ENVIRONMENTS		5. TYPE OF REPORT & PERIOD COVERED Technical Report
		6. PERFORMING ORG. REPORT NUMBER CR-82-1081
7. AUTHOR(s) Bhagwant Samyal Walter Naumann		8. CONTRACT OR GRANT NUMBER(s) DNA 001-81-C-0219
9. PERFORMING ORGANIZATION NAME AND ADDRESS Effects Technology, Inc. 5383 Hollister Avenue Santa Barbara, California 93111		10. PROGRAM ELEMENT, PROJECT, TASK AREA & WORK UNIT NUMBERS Subtask X99QAXVX000-01
11. CONTROLLING OFFICE NAME AND ADDRESS Director Defense Nuclear Agency Washington, DC 20305		12. REPORT DATE 30 June 1982
		13. NUMBER OF PAGES 68
14. MONITORING AGENCY NAME & ADDRESS(if different from Controlling Office)		15. SECURITY CLASS. (of this report) UNCLASSIFIED
		15a. DECLASSIFICATION/DOWNGRADING SCHEDULE

16. DISTRIBUTION STATEMENT (of this Report)

Approved for public release; distribution unlimited

17. DISTRIBUTION STATEMENT (of the abstract entered in Block 20, if different from Report)

18. SUPPLEMENTARY NOTES

This work was sponsored by the Defense Nuclear Agency under RDT&E RMSS Code B323081466 X99QAXVX00001 H2590D.

19. KEY WORDS (Continue on reverse side if necessary and identify by block number)

Data Acquisition	Magneto-optic Sensor	Underground Test
Data Link	Pockels Effect	Nuclear Weapon Effects Test
Fiber Optic	Faraday Effect	Measurement of Electromagnetic Fields
Electro-optic Sensor	Satellite Testing	Instrumentation for UGT

20. ABSTRACT (Continue on reverse side if necessary and identify by block number)

Electro-optic and magneto-optic sensors for measurement of SGEMP-induced electromagnetic fields in and around a satellite in a UGT environment and a fiber optic data link suitable for relaying analog measurements inside the satellite to outside data collection devices are described. The electro-optic and magneto-optic sensors are based on the Pockels and Faraday Effects, respectively. The former has a sensitivity range of $10^2 - 10^6$ v/m and the latter $1 \times 10^{-6} - 34 \times 10^{-4}$ Weber/m^2. Brief theoretical reviews and optical

DD FORM 1473 EDITION OF 1 NOV 65 IS OBSOLETE

UNCLASSIFIED

20. ABSTRACT (Continued)

systems for the application of these sensors are presented. These sensors have several advantages over the conventional electrical sensors and they exhibit a great potential for measurement of electromagnetic fields. However, the effects of radiation on these sensors are uncertain and need to be assessed for any future development of these sensors. The fiber optic data link consists of several transmitter modules, located at the satellite, connected by optical fibers to the corresponding receiver modules located at a radiation safe alcove. The link features (1) recovery of the transmitter module circuitry from the radiation-induced effects in less than one cycle of the data to be recorded, and (2) FM or digital transmission of the data over the optical fibers. Existing DNA owned DES formatters may be used with this link to eliminate the unnecessary development costs and to insure compatibility with the existing recording techniques.

TABLE OF CONTENTS

LIST OF ILLUSTRATIONS

LIST OF TABLES

LIST OF TABLES (Concluded)

SECTION 1

INTRODUCTION

This final report describes instrumentation for future satellite and missile underground nuclear tests (UGT). In particular, electro-optic (EO) and magneto-optic (MO) sensors for the measurement of SGEMP-induced electromagnetic fields on and in a satellite in an UGT environment and a Fiber Optic (FO) data link suitable for relaying remote electrical measurements inside the satellite to outside data collection devices are described. The sensors and the fiber optic data link are not used together and are intended for different applications. The EO and MO sensors use optic fibers for transmission of light but require no FO data link of any kind.

The work in this report commenced with solicitation of information on EO and MO sensing materials, modulators and possible existence of sensors for measurement of electromagnetic fields from various vendors. Simultaneously, a library literature survey and a DNA document search was launched for the above information. No commercially available EO and MO sensors for the measurement of electromagnetic fields have been found. The literature survey did cite the possible applications of the Kerr effect, Pockels effect and Faraday effect for measurement of electromagnetic fields. The application of the Kerr effect was rejected because of the many disadvantages of nitrobenzene which exhibits the best Kerr sensitivity. The other two effects showed the best potential for application as EO and MO sensors. The FO link work and discussion is based on the past experience of Effects Technology, Inc. (ETI) in designing FO systems for DNA and others.

EO and MO effects are discussed in Section 2. The description of the EO and MO sensor systems in general and for satellite UGT in particular is presented in Subsections 3.1 and 3.2, respectively;

followed by a summary of the EO and MO sensors in Subsection 3.3 and a comparison of the EO and MO sensors versus the conventional electrical sensors in Subsection 3.4. Section 4 discusses optical fibers for use in radiation environment. The FO data link is described in Section 5.0. Section 6.0 concludes the report by discussing the advantages of the EO and MO sensors (Subsection 6.1), the problems and areas of concern for any future development of the sensors and FO data link (Subsection 6.2) and the recommendations for any required development of the sensors (Subsection 6.3.1) and the FO data link (Subsection 6.3.2).

Appendices A and B describe polarization analysis of the EO and MO systems and the design parameters of the conventional electrical sensors, respectively. A glossary of the scientific terms is included in Appendix C.

SECTION 2

ELECTRO-OPTIC AND MAGNETO-OPTIC EFFECTS

Kerr, Pockels, and Faraday effects were considered for possible application in EO and MO sensors for satellite testing in a UGT environment. Because of the many disadvantages of nitrobenze which exhibits the best Kerr effect sensitivity, the application of the Kerr effect was considered unattractive and is not discussed in this report. A brief review of the other two effects and their sensing materials is presented in this section.

2-1 POCKELS EFFECT

Pockels effect is a linear electro-optic phenomenon exhibited by certain crystals which lack a center of symmetry. An applied E-field, either parallel or perpendicular to the optic axis, depending on the crystal, produces refractive index changes which increase linearly with the field and thereby induces birefringence into the crystal. A light beam traveling along the optic axis in such a crystal experiences a differential phase delay called the retardation, Γ, due to the applied field. From the literature one finds an expression for relative phase retardation given by

$$\Gamma = 2\pi \, n_0^3 r_{ij} \, E_i \, L/\lambda_0$$

where

n_0 = refractive index o-ray

λ_0 = wavelength of light in free-space

E_i, E_e = internal and external field components

r_{ij} = electro-optic coefficients

L = optical path length in the material

7

The relative retardation, Γ, is measured as described in Section 3, and using the above expression the internal field E_i is found. Due to the complete dielectric nature of the optical system and crystal, E_i depends upon the crystal shape, the dielectric constant and the external field E_e. Using a crystal of known shape, the simpliest one being an ellipsoid of revolution about the optical propagation direction, E_e is found from the expression that describes how the E field permeates the crystal, i.e.,

$$\frac{E_i}{E_e} = \frac{D^{-1}}{D^{-1} + K - 1} \qquad (< 1)$$

The depolarization factor, D, in the direction of the applied field is obtained from literature equations as a function of the aspect ratio of the crystal i.e., the ratio of the length of the semi-major axis to that of a semi-minor axis. K is the relative dielectric constant for the internal field component E_i.

A figure of merit for electro-optic sensing materials can be written as $M = n^3 r_{ij} E_i/E_e$. Table 1 shows properties and M for two groups of materials. These materials are commercially available as high quality modulator materials and are compatible with He-Ne (663 or 1152 nm) and laser diode (820 nm) light sources.

For KDP group materials only the E-field component parallel to the optic axis produces relative retardation. The electro-optic coefficient $r_{ij} = r_{63}$ where $j = 3$ (x_3) is the field direction. KD*P and CD*A are clearly the best in the group on the basis of the figure of merit. These crystals are hygroscopic and generally temperature sensitive. An example of the sensitivity that can be achieved with a 6 mm long KD*P crystal at optical wavelength of 820 nm is considered. We assume a value of 2 for the aspect ratio, a, and obtain calculated E_i/E_e to be 0.039. For a relative retardation, Γ, of 16% we find the external field

Table 1. Electro-optic sensing materials.

Material	$r_{ij} \times 10^{-12}$ (m/V)	n_o	Dielectric Constant K	Figure of Merit $M \times 10^{-12}$ (m/V)	Comments
Potassium Dihydrogen Phosphate Group					
KDP	$r_{63} = 10.5$	1.508	$K_3 = 21$	26	
KD*P	$r_{63} = 26.4$	1.504	$K_3 = 50$	45	Large Crystals Available,
ADP	$r_{63} = 8.5$	1.522	$K_3 = 15$	24	E-Field || to Optic Axis,
RDP	$r_{63} = 15$	1.506	$K_3 = 28$	33	Hygroscopic, Temperature
CDA	$r_{63} = 16.7$	1.563	$K_3 = 34$	38	Sensitive
CD*A	$r_{63} = 36.6$	1.559	$K_3 = 61$	62	
Lithium Niobate Group					
LiNbO$_3$	$r_{22} = 7$	2.286	$K_1 = 78$	2.16	Relatively Temperature
LiTaO$_3$	$r_{22} = 1$	2.176	$K_1 = 53$	0.39	Insensitive, Handling Ease

component E_e equals 1.0×10^6 v/m, which is the maximum value expected in out application. If we further assume the lowest field to be measured is 100 v/m, then a calculated value of 0.16×10^{-4} for Γ is obtained. This estimate of Γ is reasonable and should be easily measurable using the differential detection system and the sum and difference of two orthogonal components of intensity as described in detail in Section 3.

For $LiNbO_3$ materials, a field (along x_2 or x_1 axis) perpendicular to light traveling along the optic axis (x_3) produces a relative retardation. The appropriate electro-optical coefficient in this case is $r_{ij} = r_{22}$. These materials are non-hygroscopic and relatively temperature insensitive.

2-2   FARADAY EFFECT

The Faraday effect is a linear magneto-optic phenomenon exhibited in certain glasses. A magnetic field applied parallel to a plane polarized light propagating along the optic axis in such a glass causes the optical polarization rotation of the incident light. The polarization rotation is given by $\theta = V B_e L$ where

> V = verdet constant
> B_e = applied (external) magnetic field component
> L = optical path length in the material

The expression is strictly true only for diamagnetic doped glasses and paramagnetic glasses which have values of relative permeability near that of space. In such materials, the internal field does not depend strongly on the shape of the crystal and a simple figure of merit is written as $M' = V/\alpha$ rad/G where α is the attenuation coefficient (cm^{-1}).

10

The ferromagnetic materials such as YIG have high permeability below saturation and they require a biasing field perpendicular to the opical path in order to align the inherent magnetic domains and obtain optical uniformity. Here polarization rotation is given by

$$\theta = B_1 L \frac{\theta_f}{4\pi M_s}$$

where

B_1 = internal magnetic field component

θ_f = Faraday rotation per unit length

$4\pi M_s$ = Saturation Magnetization

$B_1/B_e = D_a^{-1}$ (demagnetization factor)

The internal and external magnetic field components, B_1 and B_e, are related by a demagnetization (depolarization) factor, D_a, which is similar to that discussed previously in the Pockels effect. In this case a figure of merit is written as

$$M'' = \frac{\theta}{B_e L \alpha} = \frac{\theta_f}{4\pi M_s D_a \alpha} \qquad rad/G$$

The properties and figures of merit of some commercialy available magneto-optic sensing materials are shown in Table 2. For YIG a typical value of $4\pi M_s$ is taken from literature and D_a correponds to an aspect ratio, a, of 5. YIG is clearly the best material on the basis of the figure of merit, but the need for completely dielectric sensors may preclude its application for satellite testing. Although Hoya and Schott glasses have relatively low figures of merit, their application as magneto-optic sensors has been reported in the literature.

11

Table 2. Magneto-optic sensing materials.

Glass and TGG (λ = 633nm)

Material	Verdet Constant $V(\text{rad-g}^{-1}\text{-cm}^{-1})$	Loss α (cm^{-1})	Figure of Merit $M' = |V/\alpha|$ (rad-g^{-1})	Comments
Corning 8363	$+2.6 \times 10^{-5}$	3×10^{-3}	0.87×10^{-3}	
Dysprosium Alumina Silicate	-6.4×10^{-5}	$\sim 10^{-2}$	6.4×10^{-3}	-v for paramagnetic ions,
Hoya FR-4	-3.0×10^{-5}	3×10^{-2}	1.0×10^{-3}	+v for diamagnetic ions
Hoya FR-5	-7.3×10^{-5}	3×10^{-2}	2.4×10^{-3}	
Praseodymium Alumina Silicate	-6.1×10^{-5}	$\sim 10^{-2}$	6.1×10^{-3}	
Schott SFS-6	$+2.6 \times 10^{-5}$	1.5×10^{-3}	17.3×10^{-3}	available in any
Schott SFS-57	$+2.0 \times 10^{-5}$	2.5×10^{-3}	8.0×10^{-3}	specified shape and
Schott SFS-58	$+2.4 \times 10^{-5}$	2.0×10^{-3}	12.0×10^{-3}	size, α calculated
Schott SFS-59	$+2.6 \times 10^{-5}$	2.0×10^{-3}	13.0×10^{-3}	@ 620 nm
TGG	-13.0×10^{-5}	7.0×10^{-2}	1.86×10^{-3}	

Ferromagnetic Material (λ = 1152 nm)

Material	θ_f $(°/\text{cm})$	$4\pi M_s$ (g)	D_a	Loss α (cm^{-1})	Figure of Merit $M'' = \theta_f/4\pi M_s D_a \alpha$ (rad-g^{-1})	Comments
YIG	184	1770	0.0558	0.8	40.6×10^{-3}	best material, transparent

12

The external magnetic field component B_e is determined from a measured value of θ as described in Section 3 and using the above relations. An example of the sensitivity of a Hoya FR-5 rod 10 cm long and approximately 1 cm in diameter is considered. For a Faraday rotation θ of 2.5% the calculated B-field is 34 G (34×10^{-4} Weber/m^2), the maximum value expected in our application. The minimum value of 2θ that would be measureable is of the order 0.16×10^{-4} (same as the relative retardation in Pockels materials) which corresponds to a field value of 0.01 G (1.0×10^{-6} Weber/m^2). However, the use of YIG in this example would result in much smaller material dimensions.

ELECTRO-OPTIC AND MAGNETO-OPTIC SENSORS

Electro-optic (Pockels) and magneto-optic (Faraday) effects des-
cribed in Section 2 have been widely exploited for applications as
modulators and isolators. In such application, the required electric
fields and magnetic fields are generated by high voltage electrodes and
solenoids, respectively. For satellite testing, electromagnetic fields
already exist due to SGEMP and no external driving source for the EO and
MO sensors is required. The sensors are completely dielectric and they
do not perturb the surrounding fields being measured as much as the
conventional electric sensors. Furthermore, when the sensors are used
with fiber optic transmission, for which they are well suited, they form
optical systems which are immune to EMI and other electrical noise
sources. The EO and MO sensing materials sensors have fast time
responses approaching that of electronic lattice relaxation times (10^{-13}
to 10^{-14} seconds). Thus the optical system response is limited only by
the response of the detector and associated electronics.

In this section, electro-optic and magneto-optic systems in
general are described in Subsection 3.1 and in particular for Satellite
UGT in Subsection 3.2. Subsection 3.3 presents a summary of EO and MO
sensors. A comparison of the EO and MO sensors versus the conventinal
electrical sensors is discussed in the last Subsection 3.4.

3-1   ELECTRO-OPTIC AND MAGNETO-OPTIC SYSTEMS

Systems for measuring the relative retardation, Γ, in EO (Pockels
effect) sensors and the polarization rotation angle, θ, in MO (Faraday
effect) sensors are shown in Figures 1 and 2, respectively. In these
figures linearly polarized laser light is biased either by a quarter

LEGEND:

D   - DETECTOR
I_1, I_2 - MODULATED INTENSITY COMPONENTS
L   - LINEARLY POLARIZED LASER
M   - MIRROR
PBS - POLARIZING BEAM SPLITTER
EOS - ELECTRO-OPTIC SENSOR
W   - $\lambda/4$ RETARDATION WAVEPLATE
E   - ELECTRIC FIELD
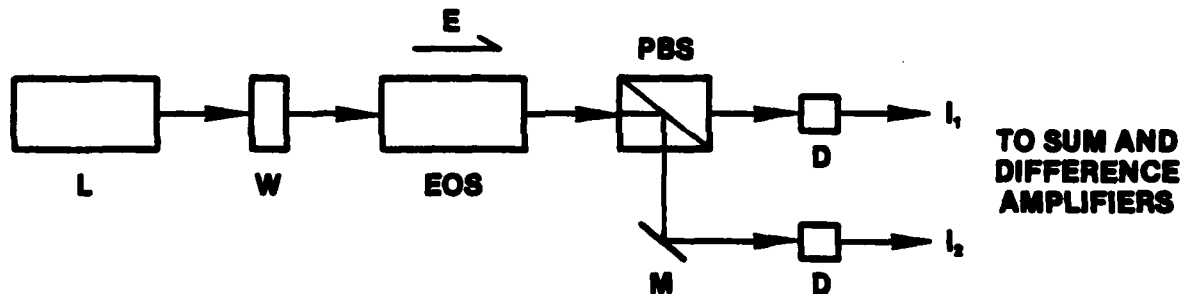
Figure 1.   Electro-optic (Pockels effect) system for measuring electric fields.

15

LEGEND:
A   - ANALYZER
D   - DETECTOR
I_1, I_2 - MODULATED INTENSITY COMPONENTS
L   - LINEARLY POLARIZED LASER
M   - MIRROR
MOS - MAGNETO-OPTIC SENSOR
B   - MAGNETIC FIELD
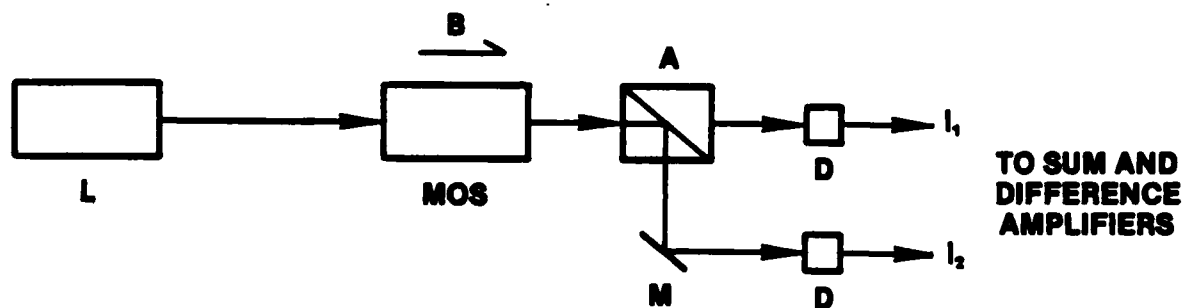
Figure 2.   Magneto-optic (Faraday effect) system for measuring
           magnetic fields.

16

wave retardation plate to give circularly polarized light or by orient-
ing the polarization at 45 to the analyzer axis such that in the
absence of the applied fields the two orthogonal components of the
intensity at the polarizing beam splitter or the analyzer output are
equal. Application of an E-field makes the EO sensor birefringent and a
B-field causes rotation of the polarization vector in the MO sensor.
The resulting unequal intensity components I_1 and I_2 are measured by two
separate detectors and fed into sum and difference amplifiers.

A straightforward polarization analysis (see Appendix A for
details) of the EO and MO optical systems yields the expression for
intensities as

$$\frac{I}{I_0} = \begin{cases} \frac{1}{2} (1 \pm \sin \Gamma) & \text{Pockels Effect} \\ \\ \frac{1}{2} (1 \pm \sin 2\theta) & \text{Faraday Effect} \end{cases}$$

where I and I_0 are the transmitted and incident intensities, respec-
tively. Then in terms of the ratio of difference to sum of the two
orthogonal components I_1 and I_2 of the intensity, the above expression
gives

$$\frac{I_1 - I_2}{I_1 + I_2} = \begin{cases} \sin \Gamma \; Z \; \Gamma \quad (\Gamma \ll \pi/2) & \text{Pockels Effect} \\ \\ \sin 2\theta \; Z \; 2\theta \quad (\theta \ll \pi/4) & \text{Faraday Effect} \end{cases}$$

This ratio directly provides a measure of the relative phase retard-
ation, Γ, and Faraday rotation, θ, in the EO and MO sensors, respec-
tively. The limitations of Γ and θ stated, in parenthesis above,
dictate the ranges over which the sensors operate linearly. The

measured values of Γ and θ are used in the appropriate expressions described in Section 2 to calculate the corresponding E- and B-field components.

3-2   EO AND MO SYSTEMS FOR SATELLITE UGT

Figure 3 shows a schematic (conceptual design) of a typical EO or MO sensor for satellite testing in an underground nuclear environment. The sensor along with its passive optical components is located at the measurement site.   The light source, the optical receiver and electronics are located at a relatively radiation safe alcove.   Light is transmitted to and back from the sensor by means of optical fibers.

A detailed optical system utilizing EO or MO sensors for satellite UGT is shown in Figure 4. The labels are identified in the legend. One optic fiber transmits light to the sensor and two fibers bring the modulated irradiation of two orthogonally polarized components of light to the alcove where they are measured by the detectors. The signals (photocurrents) from the detectors are fed to the difference and sum amplifiers and the resulting two analog signals are recorded.

Three sensors, one for each component of the electromagnetic field, oriented in mutually perpendicular directions are required to determine the E- or B-field completely.   The number of optic fibers required can be reduced by splitting the light from one source into two incident beams, at the measurement site, for two different sensors. All the fibers can be in one bundle if desired, but this would not result in any significant overall weight reduction. It may be pointed out that no FO data link of any sort is needed for the EO and MO sensors. As shown in Figures 3 and 4, the signal transmitted and received at the alcove remains optical throughout.

18

SENSITIVE MATERIAL AND
OPTICAL COMPONENTS

MEASUREMENT SITE

FIELD SENSOR

OPTIC FIBERS

ALCOVE

ELECTRONICS

LASER
TRANSMITTER
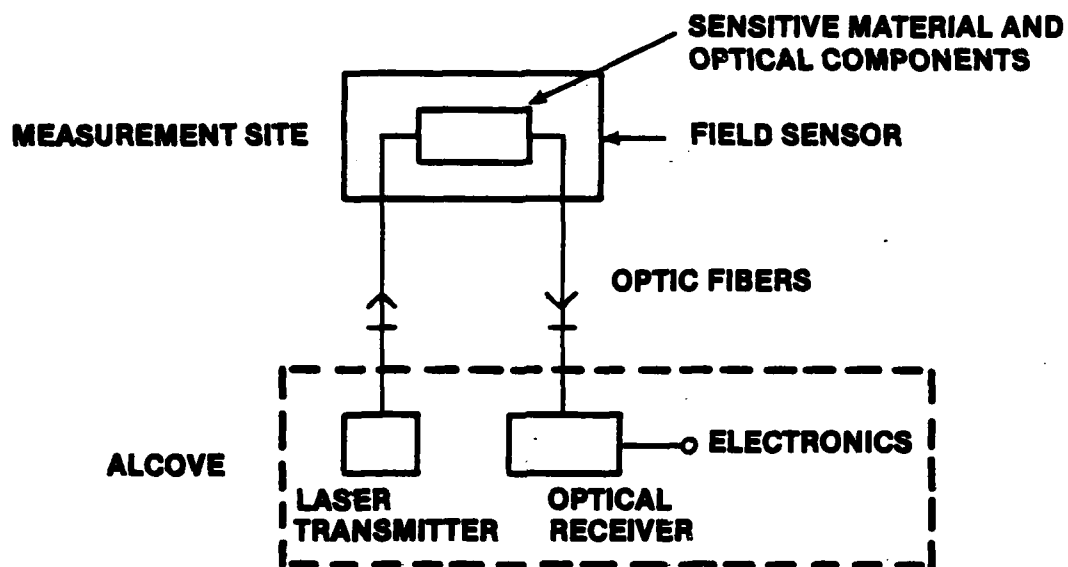
OPTICAL
RECEIVER

Figure 3. Schematic of a typical EO or MO sensor for satellite
testing in underground nuclear environment.

MEASUREMENT SITE

LEGEND:
C - FIBER OPTIC COUPLER
D - DETECTOR
L - DIODE LASER (820 nm)
P - POLARIZER
PBS - POLARIZING BEAM SPLITTER
W - $\lambda/4$ WAVEPLATE
I_1, I_2 - MODULATED INSENSITY COMPONENTS
EOS - ELECTRO-OPTIC SENSOR

100m

TO SUM AND
DIFFERENCE
AMPLIFIERS

ALCOVE
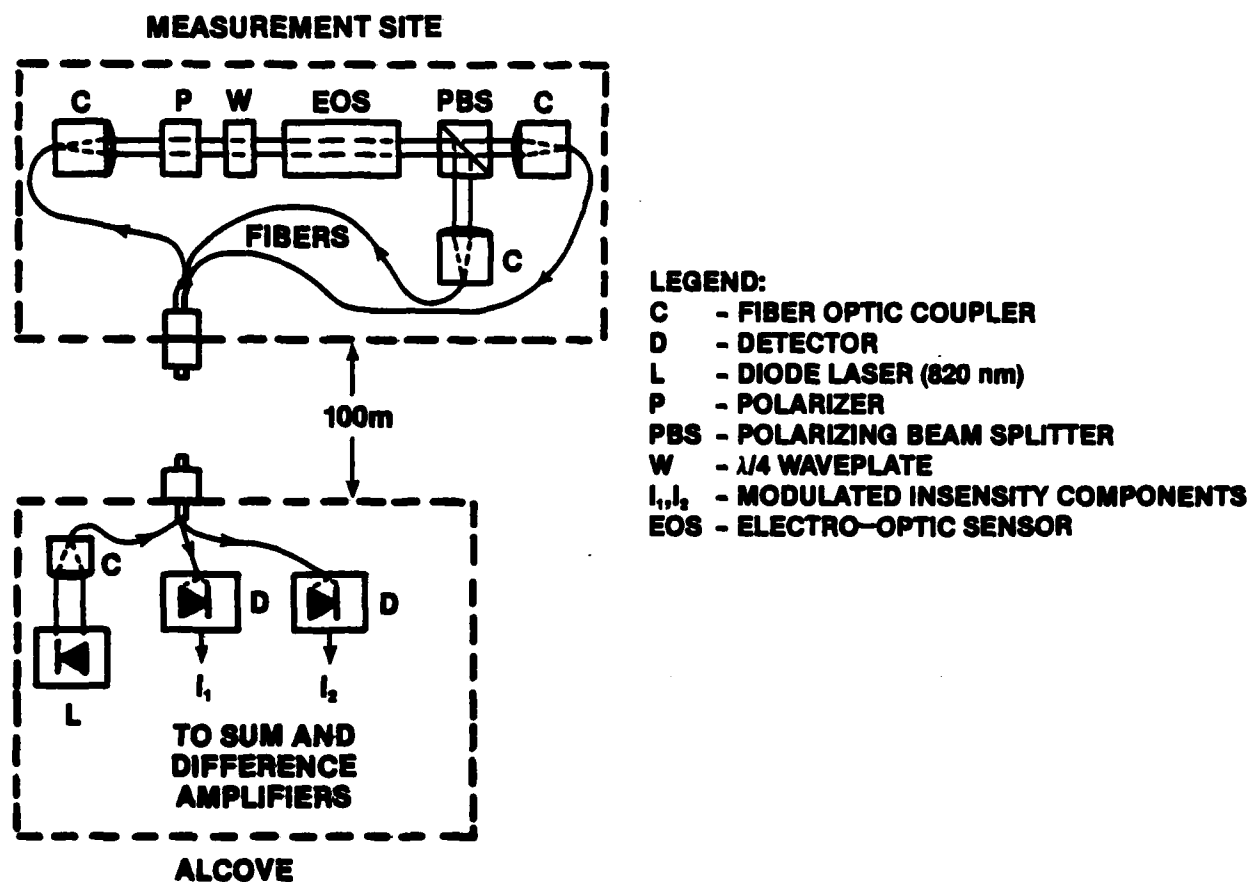
Figure 4.   Optical system utilizing EO sensor for satellite UGT.
(MO sensor is similar)

20

3-3   SUMMARY OF EO AND MO SENSORS

Electro-optic and magneto-optic sensors described in the previous sections are summarized in Table 3. The stated sensitivity figures are based on numerical examples presented in Section 2 and are considered reasonable for the dimensions of the sensing materials considered. No electrical wires or electrodes are employed in the sensors. The optical source for these sensors can be either a He - Ne laser (633 nm or 1152 nm line) or a diode laser (820 nm).

For EO (Pockels effect) sensor, KD*P is readily available commercially and has the second best figure of merit (see Table 3), but it is hygroscopic and requires a careful sealing. Besides, it is temperature sensitive. $LiNbO_3$ has a relatively low figure of merit, but it is temperature insensitive and nonhygroscopic. Both of these materials suffer from internal field relaxation when subjected to very low frequency (< 60 Hz) fields or high temperatures. Fortunately, the above two environmental constraints (high temperature and low frequency fields) are not present in satellite UGT.

Among the MO (Faraday effect) materials YIG has the best figure of merit (see Table 2). The use of YIG as a MO sensing material results in small practical dimensions of the sensor. But YIG requires a biasing (either dc or a permanent magnet) field perpendicular to the optical axis, as described earlier. Therefore, its use in the satellite UGT may be objectionable. Glasses are easy to use, but due to their lower sensitivity, longer lengths are required to obtain acceptable Faraday rotation measurements.

A differential detection system and the ratio of difference to sum of two orthogonal components of the intensity are employed in both the sensors. The lowest intensity modulation index (i.e., Γ or 2θ) that would be measureable by these sensors is of the order 0.16×10^{-4}. The

21

Table 3. Summary of electro-optic and magneto-optic sensors.

Sensor	Measurement	Sensitivity	Drive Mechanism	Sensing Material Shape	Optical Source	E.O/M.O Sensitive Material	Problems	Detection	Time Response	Comments
E.O. (Pockels effect)	E-Field	$10^2 - 10^6$ v/m	existing field	crystal	He-Ne Laser (633 nm) Diode Laser (820 nm)	LiNbO$_3$	Temp. Sensitivity	Direct, 2 Photo Detectors	$10^{-13} - 10^{-14}$ s	E Field Along x$_1$ or x$_2$ transverse axes
							Internal Field Relaxation			E Field Along the optic x$_3$ axis
						KD*P	System Calibration Required			
M.O (Faraday effect)	B-Field	$1 \times 10^{-6} - 34 \times 10^{-4}$ weber/m^2	existing field	circular rod		Various Glasses TGG & YIG	YIG Transparent to IR only			B-Field ‖ to light Propagation
										YIG Best Material

22

EO and MO sensing materials have very fast time responses (10^{-13} to 10^{-14} seconds) and there is hardly a need to consider their frequency responses. Thus, the response of the optical system (sensor) is limited only by the response of the detector and associated electronics.

3-4   EO AND MO SENSORS VERSUS CONVENTIONAL ELECTRICAL SENSORS

A comparison of the EO and MO and conventional electrical sensors is presented in Table 4. The parameters of the EO and MO sensors are described in the previous sections. The information on the conventional electrical sensors is taken from Appendix B where separate tabulated parameters of each of the sensors are presented. The abbreviations, in parentheses, underneath a sensor type stand for various sensor systems that are described individually in the appendix. For example, underneath D-DoT sensor, HSD stands for hollow spherical dipole. The quantities denoted by an asterisk in Table 3 do not pertain to one sensor system, but are representative of all the systems for a particular sensor described in Appendix B.

Table 4 shows the time responses of the EO and MO sensor materials to be faster by several orders of magnitude than the responses of the corresponding electrical E-field and magnetic field (B) sensors. However, the detectors, amplifiers and recorders limit the responses of the EO and MO sensors at present. The sensitivities of the EO and MO sensors are arrived at by considering reasonable dimensions of the appropriate sensing materials; for the electrical sensors the equivalent area or length, A_{eq} or L_{eq}, are obtained from Appendix B. Certain other parameters such as figures of merit are not directly comparable for the two kinds of sensors and therefore, are not shown in the table.

Table 5 lists some of the advantages of the EO and MO sensors over the corresponding electrical sensors. These completely dielectric EO and MO sensors exhibit a great potential for measurement of electro-

Table 4. Comparison of EO and MO sensors and conventional electrical sensors.

Sensor Type	Field Qty. Measured	Size/Shape	Rise Time or Frequency Response	Sensitivity or Eq. Area/Length	Sensor Material
EO (Pockels Effect)	E	Crystal, Circular Rod Disc	$10^{-13} - 10^{-14}$ s	$10^{-2} - 10^6$ V/m	Dielectric
MO (Faraday Effect)	B	Circular Rod		7×10^{-6} 34×10^{-4} Weber/m^2	Dielectric
D – DOT (HSD,ACD,EPD,CFD)	$\dot{D}$	(SED) Small Electric Dipole Rad. a = 3–10(m)	*Tr = 1–3 ns *$\leq$ 500 MHz to $\leq$ 8 GHz	*A_{eq} = 10^{-4} to 0.001 m^2	Metal
E-Field (PPD, PMD)	E	SED	*Tr = 0.1 – 0.5ns	*L_{eq} = 0.005 – 0.6	Metal
Magnetic Field (CML,MGL,OML,MTL)	$\dot{B}$	LOOP	*Tr = 0.2 – 5ns *$\leq$ 3 MHz to $\leq$ 330 MHz	*A_{eq} = 10^{-5} → 0.2m^2	Metal
I – DOT (CPM,OMM,SMM, IlI – I – dot – 1)	$\dot{I}$	Inductive Loop, Gap Moebius Loop	*Tr = 0.3 → 3ns		Metal
Current CPM	I	One-turn Transformer	*4KHz → 500MHz		Metal

* The values are representative of many systems for a particular sensor described in Appendix B.

24

Table 5. EO and MO sensors versus conventional electrical sensors.

EO and MO Sensors

1. Completely dielectric; not as perturbing to the fields being measured.

2. Eliminate breakdown in high radiation source region.

3. Amenable to optic fiber transmission; immune to RFI and other noise sources.

4. Sensing materials exhibit fast time responses (10^{-13} to 10^{-14} sec).

5. Frequency response limited only by the response of detector and associated electronics.

6. Simple design.

7. Relatively inexpensive to build.

Conventional Electrical Sensors

1. All metallic; distort the fields being measured.

2. Breakdown in high radiation source region.

3. Coaxial cable transmission; susceptible to RFI and electrical noise sources.

4. Time response of the order 0.3 to 3ns, differs from sensor to sensor.

5. Frequency response of the order 4 KHz to 800 MHz, differs from sensor to sensor.

6. Usually complicated design.

7. Costly to manufacture.

magnetic fields. The need for accurate measurement of electromagnetic fields in UGT SGEMP environments thus provides a strong impetus for exploiting the advantages of these sensors. These advantages provide sufficient incentives for the development of the EO and MO sensors and their subsequent evaluation in nuclear radiation simulators so that their application in the actual UGT events can be relied upon.

SECTION 4

OPTICAL FIBER FOR RADIATION ENVIRONMENT

One of the attractive features of the EO and MO sensors is their amenability to optical fiber. In addition, optical fiber is now replacing wire in many military installations because of its light weight and immunity to electromagnetic interference. The general and environmental requirements, the effects of radiation and the selection of the optical fiber for the present applications are discussed here.

4-1 REQUIREMENTS

The optical fibers are well suited for use at near-infrared wavelengths. At longer wavelengths (> 1 μm) optical fibers exhibit low absorption losses, but sensitive detectors are only recently available for use at these wavelengths. Unlike the conventional copper wire and coaxial cable, optical fiber is completely dielectric and is not subject to disruptions by electric fields from nearby signal links or by large pulse of electromagnetic energy that accompany nuclear explosions.

A portion of the optical fiber at the measurement site shall be exposed to ionizing radiation, mostly x-rays and γ-rays, which may damage the fiber. Furthermore, the fiber shall have to meet the stringent requirements of (1) insensitivity to radiation-induced transient darkening and (2) transmission of high frequency, fast rise time optical data during the fiber darkening. The optical fiber must be capable of transmitting optical data within a few nanoseconds after the arrival of the pulsed radiation. The effects of radiation impose severe constraints on the performance of the optical fibers, these effects are discussed in the next subsection.

4-2 RADIATION EFFECTS

The optical fibers are subjected to darkening effects when exposed to pulsed and steady state ionizing radiation. Investigation of the effects of ionizing radiation on optical fibers, both for transient and steady state radiation, is of relatively recent interest and the information available from literature is often conflicting. For the application (UGT environment) considered here, the effects of transient radiation on the optical fibers are of prime concern.

The objective is the assessment of the effects of radiation on fibers so that the best fiber can be selected. The fiber shall exhibit fast recovery after exposure to pulsed radiation. In other words, the fiber shall be least susceptible to degradation from either luminescence (primarily of Cerekov origin) and transient darkening effects. Some of the important results from literature on ionization radiation and its effects on optical fibers are qualitatively stated below:

1. Electron and x-ray excitation of fibers is expected to yield equivalent results (absorption or loss in fibers) when scaled on the basis of ionizing dose.

2. Neutron-induced transient luminescence is significantly below gamma-induced transient luminescence on an absorbed dose basis.

3. Radiation conditions depend upon (a) level of radiation, (b) rate at which radiation is delivered and, (c) distribution of radiation on the fiber.

4. System performance (fiber, fiber link, source, detector) depends upon the specification of (a) fiber length, (b) data rate, (c) modulation format, and (d) operating temperature.

5. For pulsed radiation the maximum induced transient loss decreases significantly with increasing temperature.

6. Magnitude of radiation darkening depends upon the composition of the fiber and the fiber fabrication technique.

7. The transient darkening (in dB/km) varies linearly with radiation dose at least into the 10^3 to 10^4 rad (si) range.

8. For step-index fibers, PCS for example, the bandwidth is of the order 10-20 MHz-km. These fibers have a general problem of low bandwidth.

9. The PCS fibers have been found to be least sensitive to radiation-induced absroption during the first 50-1000 ns of pulsed radiation.

10. In graded-index optical fibers the signal bandwidth can be decades above the step-index variety. The bandwidth of graded-index fibers is up to 1500 MHz-km and they have insignificant mode dispersion.

11. A high bandwidth fiber IVPO, phosphorous doped internal process, exhibits the least transient darkening, about 25 dB/km, at 50 R (roentgen).

4-3   SELECTION OF OPTICAL FIBERS

It is concluded from Subsection 4.2 that no fiber has the acceptable darkening in the first 5-10 ns of the pulsed radiation so as to be usable directly in the EO and MO sensors for the measurement of transient electromagnetic fields. The optical fibers for this application

would require shielding 5-10 meters of the radiation-exposed fiber with SiO_2 to reduce the level of radiation. The required radiation dose and the corresponding fiber shield thickness that would reduce the darkening effect to approximately < 8 dB/km after irradiation of the fiber with a fast (~ 3-4 ns) radiation pulse needs to be investigated. At ETI an existing computer code can be used for this purpose.

The selection of a PCS fiber would provide a bandwidth of 50-100 MHz, on the basis of 0.2 km fiber length required between the measurement site and alcove. Alternatively, a 5-10 meters of high bandwidth fiber (graded-index) spliced at either end with PCS fiber could be used at the measurement site. The average loss across the individual splices is of the order 0.46 dB (10%). For a length of 0.2 km, a graded-index fiber would provide up to 7.5 GHz bandwidth. Both the PCS and graded-index fibers with attenuation in the range 1-6 dB/km at 850 nm wavelength are readily available commercially.

In summary, the optical fiber for use with the EO and MO sensors would require shielding over a portion of 5-10 meters at the measurement site to reduce the radiation-induced transient darkening. The shielding thickness required for the acceptable attenuation in the fiber needs to the assessed. Laboratory tests and evaluation of the fiber for recovery from radiation-induced transient darkening would prove indispensible for any required development of the sensors.

SECTION 5
FIBER OPTIC DATA LINK

In SGEMP tests of satellites a need exists for transmitting data on satellite functions during the test. The data transmission can best be accomplished using a fiber optic data link. The requirements for this link will be listed and then features of a suggested link will be described.

5-1 REQUIREMENTS

The environment includes several significant factors. Large electromagnetic fields are, of course, present. Large electric potentials will be applied to the satellite in order to assess charging effects. Displacement damage from neutrons as well as ionizing radiation damage is present.

The first requirement to be considered for a data link is the presence of electric potentials and fields. These rule out the use of electrical conductors and require that either the data be stored at the measurement site or transmitted electromagnetically through a dielectric media. Storage of data requires more power and space so transmitting the data was selected. Transmission through antennas would result in distortion of the SGEMP fields due to the antenna presence. Optical beams can be obtained from small sources and transmitted through completely dielectric optical fibers which are immune to electromagnetic interference. While a direct interface between an optical beam and a fiber is possible, fiber optic coupling was selected to avoid alignment and colimation problems.

The space inside the satellite will be limited and, therefore, battery powered circuitry is essential. In addition, the requirement of radiation hardening all the circuits in the satellite indicates that the

31

satellite instrumentation must be as small and as simple as possible. Therefore, data acquisition and storage will be done in a remote radiation safe alcove.

The radiation environment is such that permanent damage of electronic components due to neutrons is not significant. Gamma and x-ray radiation likewise will not permanently damage properly designed electronics, however, it can cause long term damage to the optical fibers. The attenuation produced in the fibers means analog transmission should be rejected in favor of FM or digital transmission.

Circuits must recover from transient effects of ionizing radiation in time to transmit the data. Recovery within approximately one microsecond of irradiation is required and is achievable.

The data to be transmitted can be accomodated with sampling rates of 1 M sample/s or less.

5-2   FEATURES

The recommended data link consists of several transmitter modules, located at the satellite measurement site, which are connected by optical fibers to the corresponding receiver modules at an alcove. Additionally, the required interface and data acquisition equipment is located in the alcove.

The transmitter modules are as simple as possible. They would eventually use hybrid construction techniques where required to minimize space, although initial units would be of conventional construction. Each module would acquire data from one or a few measurement points and transmit it over a single fiber. Figure 5 is a block diagram of a transmitter module. Data transmission is continuous with no critical timing requirements.
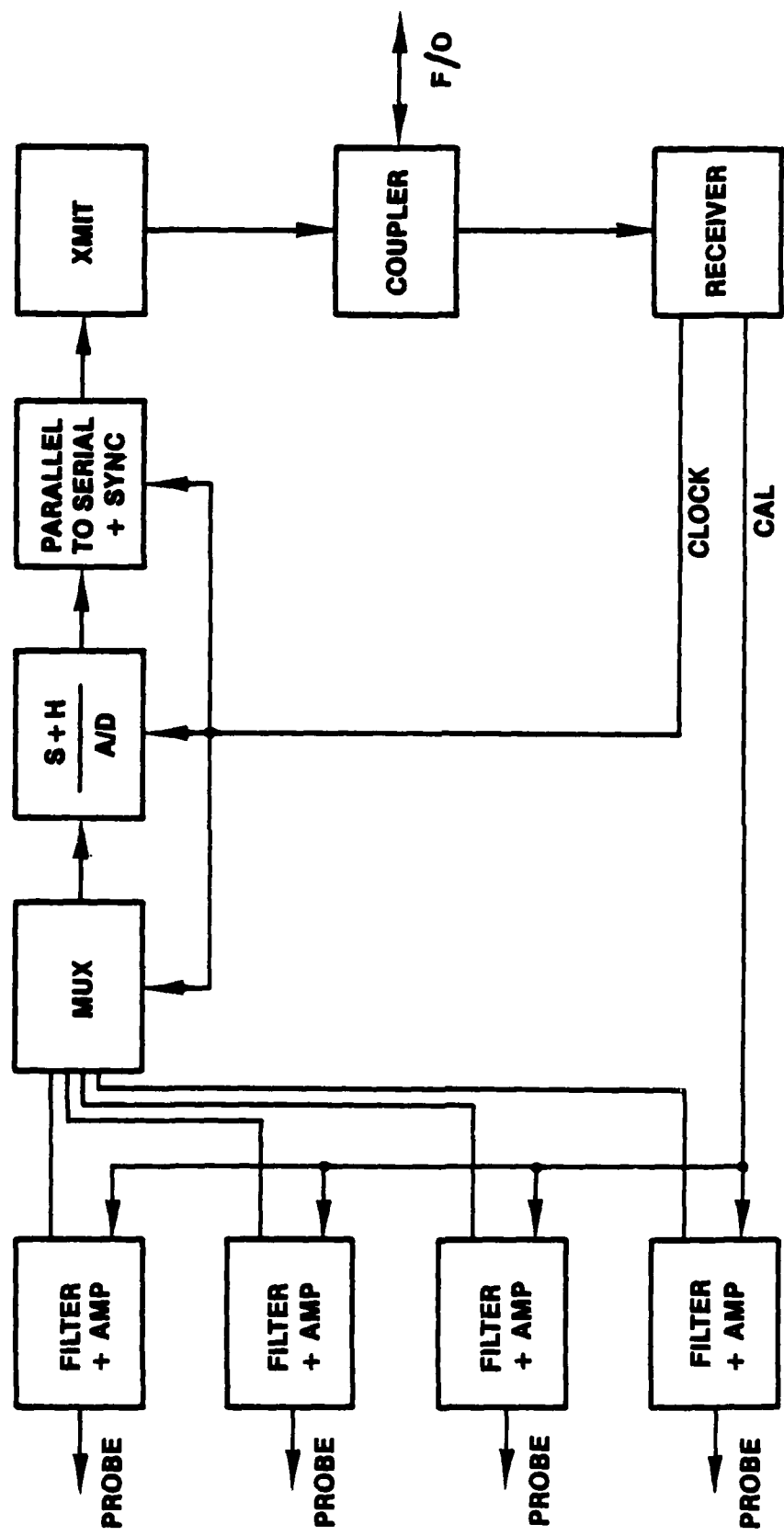
32

Figure 5. Block diagram of transmitter module in satellite.

33

Clock, turn on and calibrate information is carried to the transmitter module and pulse code modulated data is carried back to the receiver module along a single optic fiber by means of an optical directional coupler. The transmitter module contains several probes designed for accessing analog measurement signals without injecting added noise into the associated circuits. For simplicity, the filter and amplifier are adjustable only by hardware changes. The multiplexer (MUX) is only used if numerous low frequency data channels are preferred to one high frequency channel.

The data from the multiplexer go into a conventional sample and hold (S&H) and analog to digital (A/D) converter, followed by a parallel to serial converter which adds a frame synchronization word. A light emitting diode (LED) transmitter drives the optical fiber.

An optical directional coupler allows the data to output while the control information is simultaneously received from the alcove. The control information from the alcove provides a clock frequency which simplifies reception of the data back at the alcove and eliminates the need for a radiation hardened clock. Initiation of the clock signal will turn on the power in the transmitter unit. Since data will only be required for a few seconds, a small battery is sufficient to power the module circuitry. For the same reason, the low-powered but radiation sensitive MOS devices are not required which will simplify the task of radiation hardening the circuits. The detector diode in the satellite unit is energized continuously, but it draws essentially no current until light is received in the form of the clock signal. For long periods of data acquisition, the power comsumption can be minimized by intermittent periodic bursts of data transmission.

Calibration before and after the event can be most simply initiated by a low frequency signal superimposed on the clock data. A time delay will prevent calibration from being initiated by zero time noise.

The alcove equipment is shown in the block diagram of Figure 6. Again a directional coupler is used to allow transmission of on/off, clock and calibrate information to the transmitter module and to simultaneously receive data over a single fiber. If required, additional or alternate cross-talk isolation can be provided by optical wavelength differences or signal frequency differences, or separate fibers.

The bulk of the circuitry in the alcove is contained in the formatter. This digital encoding system formatter is an existing DNA equipment capable of taking data from up to 32 channels and transmitting it over a single channel to backup recorders in remote instrumentation trailers.

The interface to the existing DES formatter is accomplished in a separate chassis. In addition to the fiber optic couplers, transmitters and receivers this unit generates the clock and timing signals required by the satellite units. It also decodes the data stream and stores it in a self-contained memory. Timing signals terminate the storage of data and and an interlock prevents inadvertent erasure of the memory. The sequence of events is shown in Figure 7 which is taken from the DES operating manual.

Figure 8 shows the DES block diagram. For the recommended satellite use, the four channel encoders will be replaced with the previously described fiber optic system.

Several alternatives exist which may be found during the early development to be optimum. These include the use of separate fibers in place of the directional couplers and the use of the latest digital equipment than the DES.
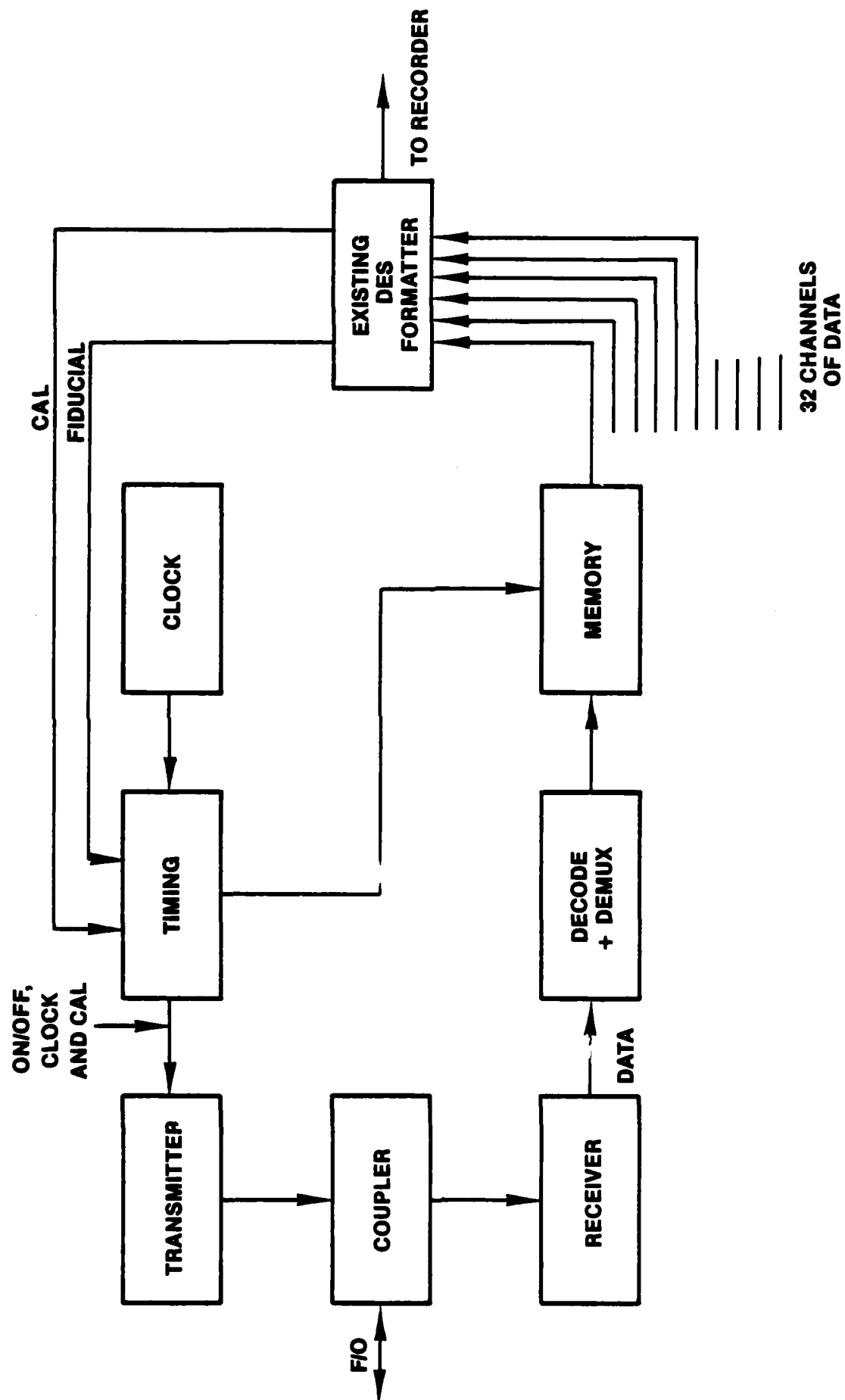
Figure 6. Block diagram of receiver module and associated equipment in alcove.

Figure 7.   System operating modes.

37
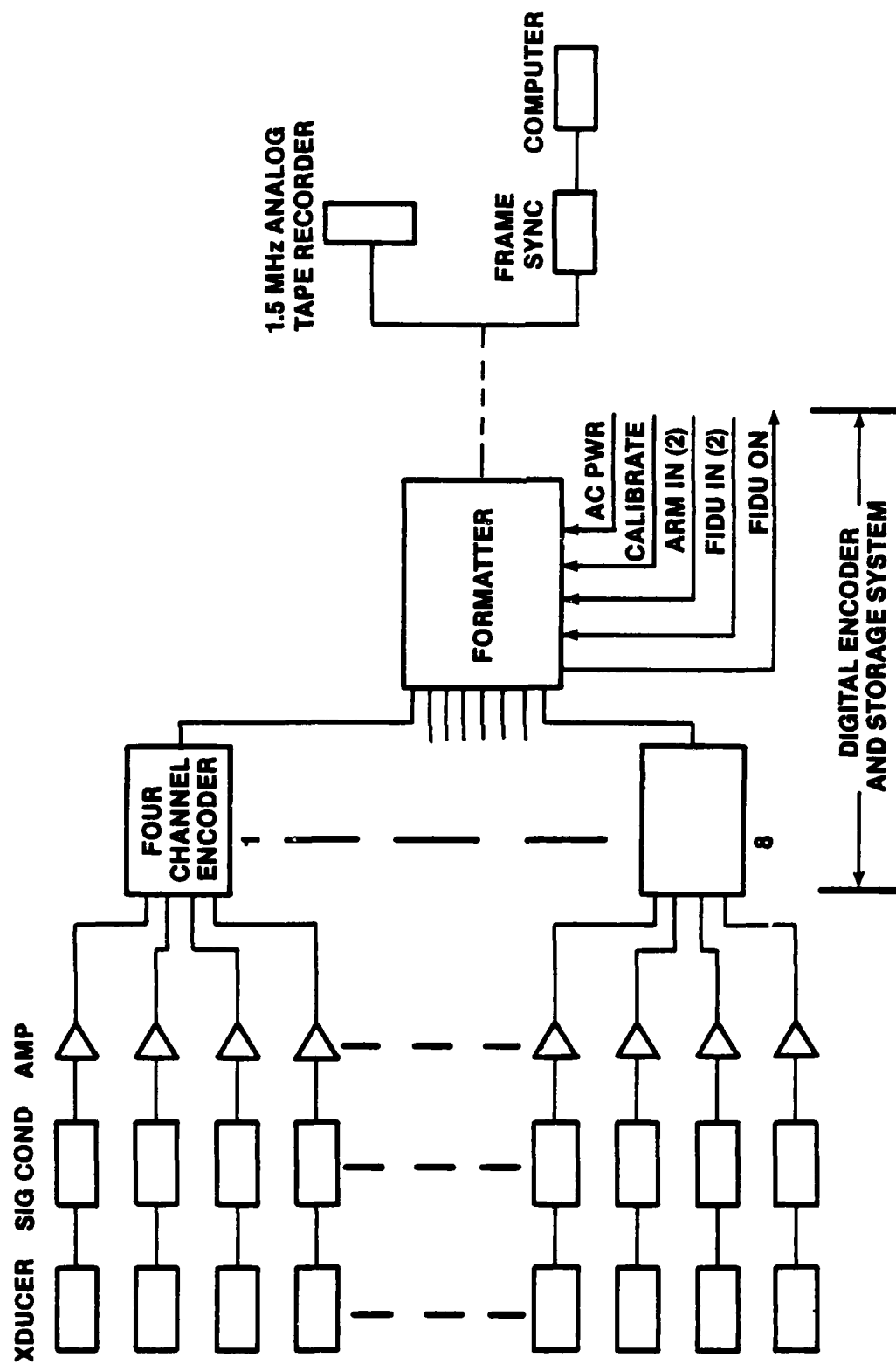
Figure 8. Block diagram of digital encoder system (DES).

In summary, the recommended system will allow extraction of data, by use of fiber optics, from a charged satellite in an SGEMP test without disruption of the E/M fields. Digital signals will circumvent fiber effects from radiation at zero time and eliminate the need for fiber shielding. The circuitry of the transmitter module in the satellite is simple, compact and battery powered and will be designed to recover from ionizing radiation-induced upset in less than one cycle of the data to be recorded. Existing DNA owned DES formatters will be used to eliminate unneccessary development costs and to insure compatibility with existing recording techniques.

SECTION 6

CONCLUSIONS

General conclusions about the advantages of the EO and MO sensors and the problems and areas of concern in the development of the sensors and FO data link are discussed in Subsections 6.1 and 6.2, respectively. The recommendations to meet the goals of any required development of the EO and MO sensors and the FO data link are presented under separate headings in Subsection 6.3.

6-1 ADVANTAGES OF EO AND MO SENSORS

Major advantages of the EO and MO sensors for the measurement of electromagnetic fields in an UGT environment are listed here.

1. The sensors are completely dielectric and they are not as perturbing to the fields being measured as the conventional electrical sensors.

2. The sensors do not breakdown in a high radiation source region because of the complete absence of any wire or cable.

3. The sensors are well-suited for use with optical fibers which are immune to electromagnetic interference and other noise sources.

4. The time responses of the EO and MO sensing materials approach the electronic lattice relaxation times (10^{-13} to 10^{-14} sec.). Therefore, the time responses of the sensors are limited only by the responses of the detectors and associated electronics.

5. Because of the fast time responses of the linear electro-optic and magneto-optic sensing materials, their frequency responses need hardly be considered.

6. The transmitters, receivers, and associated electronics of the sensors are located in a relatively radiation safe alcove and, therefore, need no radiation hardening.

7. Optical fibers are used for the transmission of light in the sensors, but no FO data link of any kind is needed.

8. The sensors are simple in design and easy to build.

9. It is relatively inexpensive to build these sensors.

6-2 PROBLEMS AND AREAS OF CONCERN

Problems that need to be addressed in any future development of the sensors and the FO data link are as follows:

1. If KD*P is used as EO sensing material, then means need to be devised to compensate for its sensitivity to temperature. However, this may not impose any severe restriction since the temperature of the environment in the satellite UGT remains fairly constant.

2. Use of glass as a Faraday rotator in the MO sensor would require long material length ($\sim$ 10cm) and may result in high absorption loss α (cm^{-1}) for certain optical wavelengths. These losses shall need to be determined experimentally for any sensor development.

3. There is insufficient information on the effects of ionizing radiation on the EO and MO sensing materials. These effects can only be assessed fully in laboratory simulated radiation environment.

4. The EO and MO sensors shall require calibration with and without the presence of simulated radiation source environment. Therefore, experimental sensors are needed for test evaluation and calibration.

5. The FO data link concept is feasible. But information on space available, number of signals to be measured and their characteristics has not been established.

6. Necessary radiation hardened circuits for the FO data link are not yet available.

6-3 RECOMMENDATIONS

Two sets of recommendations are presented here. The first set for the EO and MO sensors and the second for the FO data link.

6-3.1 Recommendations for EO and MO Sensors

The recommendations, in the form of a program plan, for any required development of the EO and MO sensors are presented below:

1. Review the requirements for the E- and B-field sensors to be used in the coming DNA underground test events. In particular, determine field levels, radiation levels and sensor mounting space constraints.

2. Review the performance of the conventional electrical sensors for the measurement of electromagnetic fields to insure improved or complimentary performance of the EO and MO sensors.

3. Continue literature surveys of (a) the EO and MO sensing materials and sensors, and (b) the radiation effects on these devices and their materials.

4. Based on the above three items, select the appropriate EO and MO sensing materials and optical components that exhibit the best overall potential for success. Contact vendors and procure the desired sizes and shapes of these materials.

5. Conduct tests to determine the response of the EO and MO sensing materials to pulsed ionizing radiation in simulators. Conduct laboratory measurements, where required, to determine optical absorption losses and temperature sensitivity of the materials.

6. Design experimental sensors and test evaluate their performance in measuring the applied E- and B-fields both with and without the presence of simulated pulsed radiation. Perform the required calibration of the sensor systems.

7. Build prototype sensors for use in the next (1983) UGT event. These sensors would be of the size and configuration that meet the requirements for use in satellite measurements. Perform qualification tests in laboratory and radiation simulators.

6-3.2 Recommendations for FO Data Link

The recommendation for any required development of the FO data link for the measurement of electrical functions of a satellite, subjected to tests in an UGT, are as follows:

1. Establish with the aid of DNA the quantity of signals and their characteristics which require measurement in satellite UGT tests.

2. Perform literature surveys, analyses and tests in laboratory and radiation simulators to assess radiation hardness of electronic and fiber optic components.

3. Design, build and test prototype FO data links for proof tests in an UGT.

REFERENCES

1. G.A. Massey, D.C. Erickson, and R. A. Kadlec, "Electromagnetic Field Components: Their Measurements Using Linear Electro-optic and Magneto-optic Effects", Applied Optics, Vol 14, 11 Nov (1975).

2. G.A. Massey, J. C. Johnson, and D. C. Erickson, "Laser Sensing of Electric and Magnetic Fields for Power Transmission Applications", SPIE, Vol. 88 Polarized Light (1976).

3. D.C. Erickson, "The Use of Fiber Optics for Communication Measurement and Control with High Voltage Substations", IEEE Trans. Power Appra. and Sys., Vol. PAS-99, No. 3, May/June (1980).

4. Glen J. Morris and Frederick D. Tart, "An Electro-optic EMP E-Field Sensor", DNA 3609P-2, Joint EMP Tech. Meeting, (NEM 1973), Proc. Vol. II, Instrumentation.

APPENDIX A

POLARIZATION ANALYSIS

POLARIZATION ANALYSIS

A)   Pockels Effect

Figure A.1 shows an ADP or KDP crystal with an electric field
applied along the Z axis and placed between a quarter waveplate and a
polarizing beam splitter. The linearly polarized light incident upon the
1/4 - waveplate is transformed into a circularly polarized beam. In the
presence of the applied E_z the principal dielectric axes are x' and y'
axes. The light incident on the crystal has equal components of E along
x' and y'. This results in the intensity components I_1 and I_2 of the trans-
mitted light in the x and y direction, respectively at the polarizing beam
splitter to be unequal. The complex amplitudes of $E_{x'}$ and $E_{y'}$ at the out-
put of the crystal can be written as

$$E_{x'} = Ae^{i\phi}x'$$

$$E_{y'} = Ae^{i\phi}y'.$$

The differential phase delay called the retardation is defined as

$$\Gamma = \phi_{y'} - \phi_{x'}.$$

We want to find the fraction of incident light intensity transmitted in
the x and y direction at an arbitrary applied field E_z. We assume a
unity of incident intensity and take $E_{x'} = E_{y'} = 1$ at the input of the
crystal. The output intensity in the y direction is given by

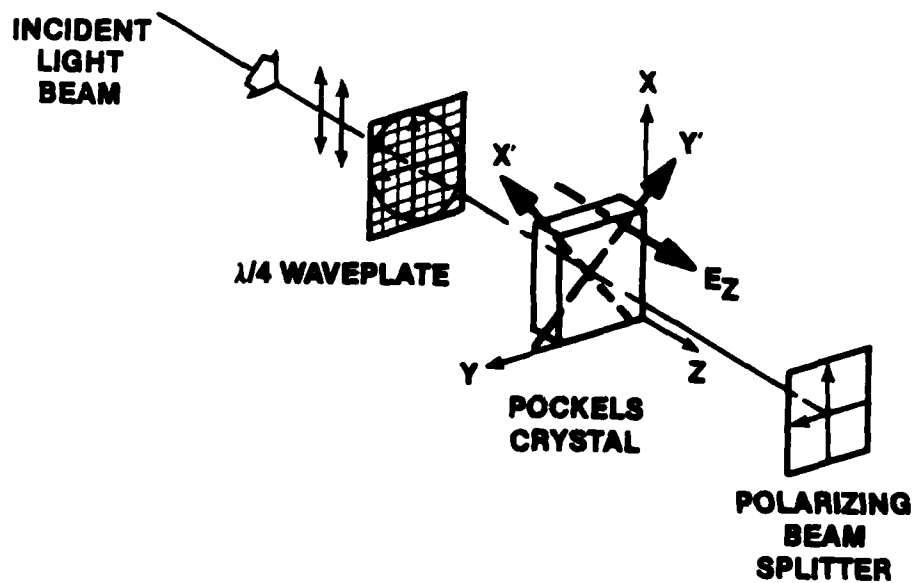$$\frac{I_{y\ trans}}{I_{incid}} = \frac{I_2}{I_o} = 1/2\ E_y E_y^*$$

A-2

Figure A.1. A Pockels (linear electro-optic) effect sensor using an ADP crystal, a quarter-wave retardation plate and a polarizing beam splitter.

where $E_y^* =$ Complex Conjugate of E_y. The components of E along x and y are

$$E_y = -\cos45° \, e^{i\phi}x' + \cos45° \, e^{i\phi}y'$$

$$E_x = \sin45° \, e^{i\phi}x' + \sin45° \, e^{i\phi}y'.$$

Substituting for E_y and E_y^* gives

$$\frac{I_2}{I_o} = 1/2 \, (-1/2 \, e^{i\phi}x' + 1/2 \, e^{i\phi}y')(-1/2 \, e^{-i\phi}x' + 1/2 \, e^{-i\phi}y')$$

or

$$\frac{I_2}{I_o} = 1/2 \left(1 - \frac{e^{i\Gamma} + e^{-i\Gamma}}{2}\right) = 1/2(1 - \cos\Gamma).$$

Similarly for the output intensity in the x direction one obtains,

$$\frac{I_1}{I_o} = 1/2(1 + \cos\Gamma).$$

If the input beam is biased by a $\pi/2$ phase retardation using a quarter waveplate, then

$$\Gamma = \pi/2 + \Gamma$$

and we get

$$\frac{I_2}{I_o} = 1/2(1 - \sin\Gamma)$$

and

$$\frac{I_1}{I_o} = 1/2(1 + \sin\Gamma).$$

Combining the above two expressions yields

$$\frac{I_1 - I_2}{I_1 + I_2} = \sin\Gamma \simeq \Gamma \quad (\text{for } \Gamma \ll \pi/2).$$

B) <u>Faraday Effect</u>

Figure A.2 shows a Faraday rotator with an applied magnetic field B parallel to light travelling along the optic Z axis and an analyzer at the rotator output. In the presence of B-field the polarization of the linearly polarized light passing through the rotator rotates through an angle θ. The intensity (irradiation) of a linearly polarized light beam is given by

$$I = \frac{C\epsilon_o E_o^2}{2}$$

Where C = Velocity of light in vacuum

ϵ_o = Permittivity of free space

E_o = Amplitude of linearly polarized plane wave

We want to determine the fraction of incident light intensity transmitted in the x and y directions at an arbitrary applied B-field. The output intensity in the x direction is given by (referring to the figure)

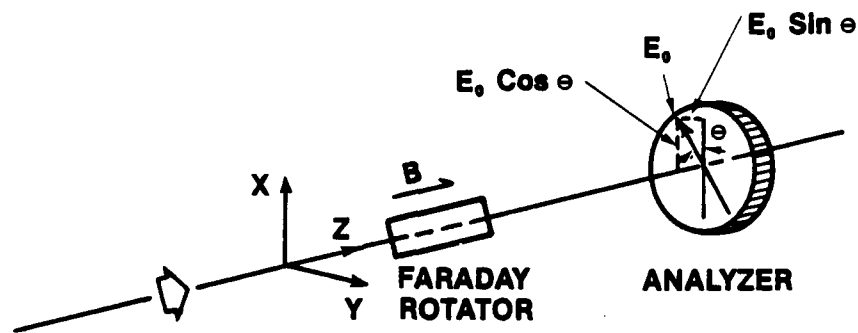$$\frac{I_{x\text{ tran}}}{I_o} = \frac{I_1}{I_o} = \cos^2\theta = 1/2(1 + \cos 2\theta)$$

Figure A.2. A Faraday (linear Magneto-optic) effect sensor
using a glass rod and an analyzer.

Where

$$E_x = E_o \cos\theta$$

$$I_o = \frac{C\varepsilon_o}{2} = E_o^2 = \text{intensity of incident light}$$

Similarly for the output intensity in the y direction one obtains,

$$\frac{I_2}{I_o} = \sin^2\theta = 1/2(1 - \cos2\theta).$$

If the polarization of the incident light is biased $\pi/4$ by rotation with respect to the analyzer, then $\theta = \pi/4 + \theta$ and we get

$$\frac{I_2}{I_o} = 1/2(1 - \sin2\theta)$$

and

$$\frac{I_1}{I_o} = 1/2(1 + \sin2\theta).$$

Combining the above two expressions yields

$$\frac{I_1 - I_2}{I_1 + I_2} = \sin2\theta \sim 2\theta \quad (\text{for } \theta \ll \pi/4).$$

References:

1. A. Yariv, 1976, "Quantum Electronics" (2nd edition), New York: Wiley. UNCLASSIFIED

2. E. Hecht/A. Zajac, 1973, "Optics", California: Addison-Wesley. UNCLASSIFIED

APPENDIX B

DESIGN PARAMETERS OF THE CONVENTIONAL
ELECTRICAL SENSORS

The design parameters of the various conventional electrical (antenna type) sensors are summarized in this appendix. The information is presented in tabular form for the various systems of a particular sensor. Separate tables on D-Dot, electric field, B-Dot, I-Dot and current sensors are included. The usual commonly used letters and symbols are used to denote the electrical quantities and sensor parameters. The information in these tables is taken from the references cited at the end of the appendix.

Table B.1. D-Dot sensors.

SENSOR SYSTEMS	FIELD QTY MEASURED	SIZES	SENSOR	TIME OR FREQ RESPONSE	SENSITIVITY (Eq Area or Length)	REMARKS
HSD-Hollow Spherical Dipole HSD-ZA(R)	$\dot{D}$	a=3 - 10 cm	Small electric dipole (SED)	tr=1-3 ns	$A_{eq}=0.01 - 0.1$ m^2	$A_{10-90} = 0.078$
ACD-Asymptotic Conical Dipole ACD-S1A(R)	$\dot{D}$		SED	<3 GHz	$A_{eq}=10^{-3} - 10^{-4}$ m^2	Cs = 1.16 pf $A_{10-90}=0.23$
FPD-Flush Plate Dipole FPD-1A	$\dot{D}$	<10 cm	SED	<500 MHz	$A_{eq}=0.01$ m^2	$A_{10-90}=0.08$
CFD-Conforming Flush Plate dipole	$\dot{D}$		SED	100 MHz	$A_{eq}=10^{-3} - 10^{-2}$ m^2	$A_{10-90}=5.3 \times 10^{-4}$

Table B.2. Electric field sensors.

SENSOR SYSTEM	FIELD QTY MEASURED	SIZES	SENSOR	TIME OR FREQ RESPONSE	SENSITIVITY (Eq Area or Length)	REMARKS
PPD-Parallel Plate Dipole PPD-1A(R)	E		SED	$tr=0.2ns + 0.5ns$ $\tau=1-100$ μsec	$l_{eq}=1$ cm	$c=200-1000$ pf
PMD-Parallel mesh Dipole PMD-1 PMD-1F	E		SED	$1.6 - 3.5$ GHz $tr = 0.1$ ns $\tau_d = 1.5$ ns	$l_{eq}=0.5$ cm → 0.6 m	$c=20$ pf

Table B.3. B-Dot sensors.

SENSOR SYSTEM	FIELD QTY MEASURED	SIZES	SENSOR	TIME OR FREQ RESPONSE	SENSITIVITY (Eq Area or length)	REMARKS
CML-Cylindrical moebius loop CML-X3F	$\dot{B}$	$\ell \sim 4cm$	loop	<30 MHz	$A_{eq} = 5 \times 10^{-4} - 2 \times 10^{-2}\ m^2$	M = 12 nH
MGL-Multigap Loop MGL-3A	$\dot{B}$	3"loop	loop & half-loop	tr=0.2 → 4.5 ns	$A_{eq} = 10^{-5} - 10^{-1}\ m^2$	$A_{10-90} = 0.24$
OML-One-conductor Many-turn-loop OML-1A(A)	$\dot{B}$		loop		$A_{eq} > 1$	
MTL-Multi-turn Loop	$\dot{B}$		loop	>2 KHz <3 MHz	$A_{eq} = 10\ m^2$ (50 turns)	N=630 nH
O3L-Octahedral Three-axis loop	$\dot{B}$	Three orthogonal components		tr=1 ns <12 MHz	$A_{eq} = 0.2\ m^2$	
RML-Rectangular Moebius loop RML-X1	$\dot{B}$		loop	<33 MHz	$A_{eq} = 5 \times 10^{-4} - 2 \times 10^{-2}$	M=12 nH Similar to CML

Table B.4. I-Dot sensors.

SENSOR SYSTEM	FIELD QTY MEASURED	SIZES	SENSOR	TIME OR FREQ RESPONSE	SENSITIVITY (Eq Area or length)	REMARKS
CPM-Circular Parallel Mutual Inductance Sensor	$\dot{I}$	d=0.1→ 2m	Inductive loop	tr=1→3ns		M=10^{-8}H
III -I-dot one-turn insertion unit	$\dot{I}$	used on 1 5/8" O.D. cable	Gap	tr=0.3ns		M=5nH
OMM-Outside Moebius Mutual Inductance OMM-1A OMM-4	$\dot{I}$	6-8 cm long ID = 10 cm →2 cm	Moebius loop	tr $\leq$ 0.5 ns > 700 MHz		Similar to CML M=2nH
SMM - Side moebius mutual inductance SMM-X1	$\dot{I}$		Moebius loop	> 800MHz tr=0.4ns		M=2nH L=4nH

B-6

Table B.5. Current sensors.

SENSOR SYSTEM	FIELD QTY MEASURED	SIZES	SENSORS	TIME OR FREQ RESPONSE	SENSITIVITY (Eq Area or Length)	REMARKS
SCI - Split core current sensor	I	D= 8-16 cm	one-turn transformer	80 bHz - 500 MHz		Clamp-on measures cable bundle currents
ICI - Inside core current sensor	I	D= 3-4 cm	One-turn transformer	5 kHz - 200 MHz		Measure pin currents
PMM - Flush Moebius Mutual Inductance	J_{total}	D ~19 cm	tr <1 ns	$A_{eq} = 10^{-2} \text{ m}^2$		M = 5 nH
FMM-1A						

B-7

REFERENCES

CONVENTIONAL ELECTRICAL SENSORS

1.   C.E. Baum, E.L. Breen, J.C. Giles, J. O'Neill and G.D. Sower, "Sensors for Electromagnetic Pulse Measurements Both Inside and Away from Nuclear Source Regions," IEEE Trans. Ant. and Prop. Vol. AP-26, No. 1, January 1978.

2.   R.H. Bonn, "Instrumentation for an Underground Nuclear SGEMP Experiment," Sensor and Simulation Notes, Note 270, 2 March 1981.

APPENDIX C

GLOSSARY OF SCIENTIFIC TERMS

ADP - ammonium dihydrogen phosphate $(NH_4)H_2AsO_4$, a crystal that exhibits nonlinear optical effects and electro-optical effects. The deuterated form $(NH_4)D_2PO_4$ is denoted AD*P.

Birefringence - the splitting of a light ray, generally by a crystal, into two components, called the ordinary and extraordinary components, with orthogonal polarization; these components travel at different velocities in different directions unless the input beam is directed along a specific direction in the crystal.

Center of Symmetry - a crystal possesses a center of symmetry if every point in the crystal can be reflected through the center to an equal distance on the other side and the resulting crystal remains identical.

CDA - cesium dihydrogen arsenate (CsH_2AsO_4), a crystal used in electro-optic modulators. CD*A is the deuterated version (CsD_2AsO_4).

Diamagnetism - the property that certain substances have of being repelled by both poles of a magnet.

Diamagnetic - having or relating to diamagnetism.

Ferromagnetic - designating a material such as iron, nickel, or cobalt having a high magnetic permeability which varies with the magnetizing force. Beyond a certain critical value of temperature, called the Curie temperature, these materials lose their high magnetic permeability and they become simply paramagnetic.

Paramagnetism - a weaker form of magnetism exhibited in certain materials when placed in an external magnetic field.

Multiplex - transmission of more than one signal within a single carrier.

Paramagnetic - designating a material such as aluminum, platinum, etc., having a magnetic permeability slightly greater than unity and varying to only a small extent with the magnetizing force.

KDP - potassium dihydrogen phosphate (KH_2PO_4), a crystal used in electro-optic modulators. The deuterated form of the crystal (KD_2PO_4) is called KD*P or D-KDP.

Kerr Effect - an electro-optic effect exhibited in certain liquids which become birefringent when placed in an electric field E. This is a nonlinear effect having quadratic variation of refractive index with applied electric field.

RDP - rubidium dihydrogen phosphate (RbH_2PO_4), a crystal used in electro-optic modulators.

TGG - terbium gallium garnet, a crystal used in magneto-optic modulators or sensors.

YIG - yttrium iron garnet ($Y_3Fe_5O_{12}$), a crystal used in magneto-optic modulators or sensors.

DISTRIBUTION LIST

DEPARTMENT OF DEFENSE

Assistant to the Secretary of Defense
Atomic Energy
    ATTN: Executive Assistant

Defense Intelligence Agency
    ATTN: DT-1B, R. Rubenstein

Defense Nuclear Agency
    ATTN: RAAE
    ATTN: STNA
4 cy ATTN: TITL
4 cy ATTN: RAEV

Defense Technical Information Center
12 cy ATTN: DD

Field Command
Defense Nuclear Agency
    ATTN: FCTT, W. Summa
    ATTN: FCTT
    ATTN: FCTT, G. Ganong
    ATTN: FCPR, J. McDaniel

Field Command
Defense Nuclear Agency
Livermore Branch
    ATTN: FC-1

Under Secretary of Def for Rsch & Engrg
    ATTN: Strategic & Space Sys (OS)

DEPARTMENT OF THE ARMY

Harry Diamond Laboratories
    ATTN: DELHD-NW-RA
    ATTN: DELHD-NW-P
    ATTH: DELHD-NW-RI, Kervis
    ATTN: DELHD-TA-L

US Army Nuclear & Chemical Agency
    ATTN: Library

US Army Test and Evaluation Cmd
    ATTN: DRSTE-EL

USAMICOM
    ATTN: Documents Section

DEPARTMENT OF THE NAVY

Naval Research Laboratory
    ATTN: Code 4773, G. Cooperstein
    ATTN: Code 2000, J. Brown
    ATTN: Code 7550, J. Davis
    ATTN: Code 6534, K. Whitney

Naval Surface Weapons Center
    ATTN: Code R40
    ATTN: Code F31

Naval Weapons Center
    ATTN: Code 233

DEPARTMENT OF THE AIR FORCE

Air Force Weapons Laboratory
    ATTN: SUL
    ATTN: CA
    ATTN: NTYC
    ATTN: NT
    ATTN: NTYP

Ballistic Missile Office
    ATTN: ENSN

Deputy Chief of Staff
Research, Development, & Acq
    ATTN: AFRDQI

Space Division
    ATTN: XR
    ATTN: YEZ
    ATTN: YGJ
    ATTN: YKM
    ATTN: YKF
    ATTN: YKS, P. Stadler
    ATTN: YNV
    ATTN: YO

Strategic Air Command
    ATTN: INT, E. Jacobsen

DEPARTMENT OF ENERGY

Department of Energy
    ATTN: Ofc of Inert Fusion, S. Kahalas
    ATTN: Ofc of Inert Fusion, T. Godlove
    ATTN: Ofc of Inert Fusion, C. Hilland

OTHER GOVERNMENT AGENCY

Central Intelligence Agency
    ATTN: OSWR/NED

DEPARTMENT OF ENERGY CONTRACTORS

University of California
Lawrence Livermore National Lab
    ATTN: L-401, W. Pickles
    ATTN: L-47, L. Wouters
    ATTN: Technical Info Dept, Library
    ATTN: L-153
    ATTN: L-153, D. Meeker
    ATTN: L-545, J. Nuckolls

Los Alamos National Laboratory
    ATTN: MS222, J. Brownell

Sandia National Lab
    ATTN: 5240, G. Kuswa
    ATTN: G. Yonas
    ATTN: 5241, M. Clauser
    ATTN: 9365, J. Allen
    ATTN: 3141

DEPARTMENT OF DEFENSE CONTRACTORS

Aerospace Corp
    ATTN: Technical Information Services
    ATTN: V. Josephson
    ATTN: S. Bower

BDM Corp
    ATTN: Corporate Library

Boeing Co
    ATTN: Aerospace Library

Dikewood Corporation
    ATTN: Tech Lib, L. Davis

EG&G Wash Analytical Svcs Ctr, Inc
    ATTN: Library

General Electric Co
    ATTN: J. Peden
    ATTN: H. O'Donnel

IRT Corp
    ATTN: R. Mertz

JAYCOR
    ATTN: E. Wenaas

JAYCOR
    ATTN: R. Sullivan

Kaman Sciences Corp
    ATTN: S. Face

Kaman Tempo
    ATTN: DASIAC

Lockheed Missiles & Space Co, Inc
    ATTN: L. Chase

Texas Tech University
    ATTN: T. Simpson

TRW Electronics & Defense Sector
    ATTN: Technical Information Center
    ATTN: D. Clement

Effects Technology, Inc
  4 cy ATTN: B. Samyal
  4 cy ATTN: W. Naumann

DEPARTMENT OF DEFENSE CONTRACTORS (Contiuned)

Lockheed Missiles & Space Co, Inc
    ATTN: S. Taimuty, Dept 81-74

Maxwell Labs, Inc
    ATTN: A. Miller
    ATTN: P. Korn
    ATTN: A. Kolb

McDonnell Douglas Corp
    ATTN: S. Schneider

Mission Research Corp
    ATTN: W. Hart
    ATTN: C. Longmire

Mission Research Corp
    ATTN: B. Godfrey

Mission Research Corp
    ATTN: B. Passenheim

Pacific-Sierra Research Corp
    ATTN: L. Schlessinger
    ATTN: H. Brode, Chairman SAGE

Physics International Co
    ATTN: A. Toepfer
    ATTN: B. Bernstein
    ATTN: C. Stallings

R & D Associates
    ATTN: W. Graham
    ATTN: P. Haas

S-CUBED
    ATTN: A. Wilson

Science Applications, Inc
    ATTN: K. Sites

Spire Corp
    ATTN: R. Little

Advanced Research & Applications Corp
    ATTN: R. Armistead